Determination of helical twist in liquid crystals: Examples and terpenoids as chiral dopants

M.P. Rosseto,[1,2] S. Hurley,[3,4] E.K. Lenzi,[1] D.-K. Yang,[3] and R.S. Zola[2,*]

[1] *Departamento de Física, Universidade Estadual de Ponta Grossa, Paraná 87030-900, Brazil*
[2] *Departamento de Física, Universidade Tecnológica Federal do Paraná, Apucarana, PR 86812-460, Brazil*
[3] *Chemical Physics Interdisciplinary Program and Liquid Crystal Institute, Kent State University, Kent, Ohio, USA*
[4] *Apple Inc, Cupertino, California 95014, USA*

(Received 18 June 2024; revised 8 August 2024; accepted 26 August 2024; published 11 September 2024)

Helical twists exist in liquid crystals as a result of the addition of chiral dopants or boundary conditions and play a role in several liquid-crystal phenomena and devices. To date, various methodologies have been explored, albeit with varying degrees of precision and complexity, often resulting in the measurement of just one parameter, such as helical sense. However, a consensus on the optimal technique remains elusive. We developed a technique to determine the total twist angle and handedness of the twist by using optical transmission spectroscopy. We present the theoretical background and experimental technique and test it against some other results and results from data published elsewhere. Furthermore, we investigate the use of three naturally occurring terpenoid materials as chiral dopants for liquid crystals and determine the helical handedness using the spectroscopy method.

DOI: 10.1103/PhysRevApplied.22.034027

I. INTRODUCTION

When a chiral dopant is introduced into a nematic liquid crystal, it induces a twisting orientation of the molecules, so that it forms a helical structure. The twist rate is defined as the pitch, P, which is the distance over which the molecules complete a full 360° rotation [1]. The ability to control this rate is crucial for many applications [2], such as in sensors, optics, and photonics, and in liquid-crystal displays, including those that transmit, reflect, and scatter light. These devices include, but are not limited to, twisted nematic (TN), supertwisted nematic (STN), polymer-stabilized cholesteric (CLC) texture (PSCT), and bistable reflective CLC [1].

The design and performance of all of these devices depend greatly on the chiral dopant used to promote the twist configuration. This dependence comes mainly from how accessible (including price), the helical twisting power (HTP), and the handedness (twist direction: right- or left-handed) of the chiral dopant. However, when the chiral nematic phase of a sample is investigated using a chiral dopant of unknown handedness and HTP, such as recently synthesized materials or even for testing naturally occurring materials, then some kind of measurement is needed to determine these parameters. Although measuring the HTP is fairly simple, with well-established methods [1], determining the helical sense remains elusive, with some techniques found in the literature, but lacking a standard procedure. Similarly, sometimes it may be necessary to determine the twist ratio of a sample, for example, in cases where the thickness is changing [3] or not previously measured, or in the cases in which chirality changes, as occurs for cholesteric liquid crystals (CLCs) under different external stimuli [4–7], and finding applications in several fields, from optics and photonics to molecular sensors [8–12]. Hence the knowledge about the number of turns inside the cell is pivotal.

In general, determining HTP is fairly simple with the help of the Grandjean-Cano wedge method [13,14]. The twisting sense, however, is not simply attainable. Unfortunately, there is no currently recognized method to determine the twisting direction based on the molecular structure [15], which is clear from the fact that a chiral dopant could induce different twisting directions depending on the nematic host [16]. Many techniques have been proposed to determine the handedness of a certain chiral dopant. Perhaps the simplest one is to mix the unknown-handedness material with a chiral dopant whose twisting sense is already known. With the HTP of both materials, it is possible to prepare two chiral nematic samples and test for miscibility [17] or to prepare a mixture of both chiral dopants aiming for a racemic mixture in case of opposite handedness and check it under the optical polarizing microscope (POM) if a compensated sample (nematic) is achieved or a sample with CLC texture is found (in case both chiral dopants have the same sense). However, this

*Contact author: rzola@utfpr.edu.br

technique is imprecise and requires a considerable amount of materials. Another method of determining the helical sense, proposed in Ref. [18], consists of measuring the position of interference lines in a wedge cell by changing the angle of the analyzer [18]. Measurement of retardation of a birefringent plate placed on a reflecting CLC cell has also been shown to determine the helical sense [19], although this method is difficult to use when the HTP is low. Last but not least, circular dichroism (CD) spectroscopy can also be used to measure the helical sense, as demonstrated in Ref. [20], but in general this measurement requires expensive equipment. Other relevant methods to determine the helical sense have been explored, especially for Lyotropic liquid crystals. For example, Tombolato *et al.* [21] used confocal microscopy to determine the handedness of chiral nematic phases formed by suspensions of rodlike viruses. Zanchetta *et al.* [22] used a method based on a numerical approach and on the Jones method for the reflection of light by chiral nematics and a small uncrossing (10°) of the analyzer to determine the handedness of chiral nematic phases of ultrashort DNA samples.

This paper describes a method for determining the handedness by measuring the transmission spectrum of the cell with a simple, portable spectrometer, which can also verify the number of turns (pitch) if the cell gap is known. Both situations require $\Delta nP \gg \lambda$, where Δn is the birefringence and λ is the wavelength of incident light. We demonstrate the use of the technique with practical examples and some already published data [23,24]. Furthermore, we tested our method to characterize some naturally occurring terpenoid materials as chiral dopants. Terpenes are major biosynthetic building blocks and are typically found in plants. Due to their hydrocarbon nature, terpenoids mix well with thermotropic liquid crystals. In fact, it has been shown before that (R)-(+)-limonene can be used as a chiral dopant, having the advantage of being very affordable when compared to synthesized materials, and acting as a natural lubricant, and hence reducing the viscosity of the nematic host [25]. Recent studies have shown that liquid crystals can detect chiral vapors from the induced structure change caused by the chiral materials, including carvone and limonene [26]. Furthermore, some terpenoids, including carvone and verbenone have been used as chiral dopants aiming for drug-delivery systems [27]. However, the aforementioned works do not measure the HTP or handedness of the materials. In this paper, we use our method to characterize three chiral terpenoids as chiral dopants: (1S)-(−)-verbenone, (3aR)-(+)-sclareolide, and (S)-(+)-carvone.

II. THEORETICAL BACKGROUND

The following section describes the method used to simulate the main equations used here. It is derived in detail in Ref. [1] for the transmission spectrum of a twisted nematic liquid crystal cell, but here, for the sake of completeness of the method, we write the main steps of the model. The inner surfaces of the cell are coated with an alignment layer with a homogeneous anchoring, where the liquid-crystal director is uniformly aligned along the rubbing direction. In a twisted cell, the liquid-crystal molecules twist at a constant rate from top to bottom substrate to match the boundary conditions, where the total twist angle is given by Φ and the twist rate is given by $\tau = \Phi/d$, where d is the cell thickness. To calculate the optical properties of such cells, the standard procedure is to divide the cell into N thin slabs of thickness $\Delta h = d/N$, where the liquid-crystal orientation is considered approximately uniform within each slab.

In the Jones representation, each optical element can be represented by a 2×2 matrix called the Jones matrix. For a twisted nematic cell, the Jones matrix can be written as

$$\vec{E}_0 = \overleftrightarrow{S}(N\Delta\sigma) \cdot [\overleftrightarrow{G} \cdot \overleftrightarrow{S}^{-1}(\Delta\sigma)]^N \cdot \vec{E}_i, \tag{1}$$

where $\vec{E}_i$ and $\vec{E}_0$ are the Jones vector of the incident and exiting light, respectively; $\Delta\sigma = \Phi/N$, $\overleftrightarrow{S}$ is the rotation matrix [1] and $\overleftrightarrow{G}$ is the Jones matrix defined as

$$\overleftrightarrow{G} = \begin{pmatrix} e^{-i\Delta\Gamma/2} & 0 \\ 0 & e^{i\Delta\Gamma/2} \end{pmatrix}, \tag{2}$$

in which $\Delta\Gamma = 2\pi(n_e - n_o)\Delta h/\lambda$, with n_e and n_o being the extraordinary and ordinary index of refraction, respectively, and λ is the wavelength of light. Now, one may define the matrix $\overleftrightarrow{B}$ as

$$\begin{aligned} \overleftrightarrow{B} &= \overleftrightarrow{G} \cdot \overleftrightarrow{S}^{-1}(\Delta\sigma) \\ &= \begin{pmatrix} e^{-i\Delta\Gamma/2}\cos(\Delta\sigma) & -e^{-i\Delta\Gamma/2}\sin(\Delta\sigma) \\ e^{i\Delta\Gamma/2}\sin(\Delta\sigma) & e^{i\Delta\Gamma/2}\cos(\Delta\sigma) \end{pmatrix}. \end{aligned} \tag{3}$$

We can now use the Cayley-Hamilton theory [28] to rewrite $\overleftrightarrow{B}^N$ as

$$\overleftrightarrow{B}^N = \delta_1 \overleftrightarrow{I} + \delta_2 \overleftrightarrow{B}, \tag{4}$$

where $\overleftrightarrow{I}$ is the identity matrix and δ_1 and δ_2 can be found through the equations

$$\begin{aligned} z_1^N &= \delta_1 + \delta_2 z_1 \\ z_2^N &= \delta_1 + \delta_2 z_2 \end{aligned}, \tag{5}$$

in which z_1 and z_2 are the eigenvalues of $\overleftrightarrow{B}$. It is, therefore, straightforward to show that

$$\overleftrightarrow{B}^N = \begin{pmatrix} \cos(\Theta) - i\dfrac{\Gamma}{2\Theta}\sin(\Theta) & \dfrac{\Phi}{\Theta}\sin(\Theta) \\ -\dfrac{\Phi}{\Theta}\sin(\Theta) & \cos(\Theta) + i\dfrac{\Gamma}{2\Theta}\sin(\Gamma) \end{pmatrix}, \tag{6}$$

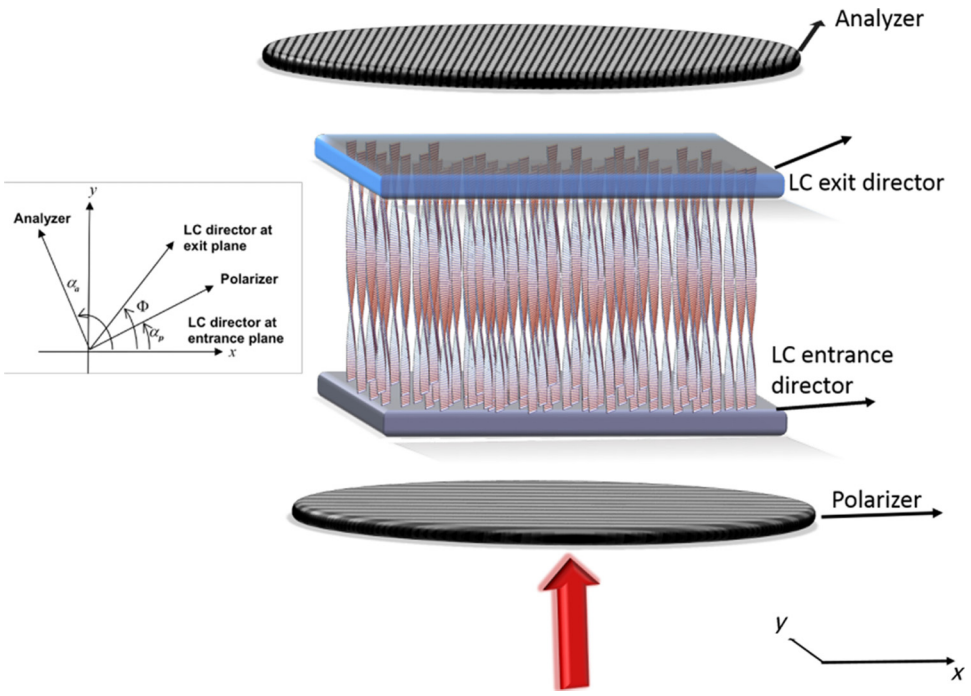

FIG. 1. Definition of the angular orientation of the cell components.

in which $\Theta = [\Phi^2 + (\Gamma/2)^2]^{1/2}$ and $\Gamma = 2\pi(n_e - n_o)N$ $\Delta h/\lambda = 2\pi(n_e - n_o)h/\lambda$.

Now, we consider the basic geometry of a liquid-crystal cell as shown in Fig. 1 where the angles are all referenced to the horizontal x axis, which is shared by the input rubbing direction. The liquid-crystal molecules twist at a constant rate from top to bottom to align with the boundary conditions, where the total twist angle, Φ, may or may not be known. However, the angles of the polarizer, α_p, and analyzer, α_a, are known. For such a geometry, the exiting field becomes

$$E_{\text{exit}} = \begin{pmatrix} \cos\alpha_a & \sin\alpha_a \end{pmatrix} \begin{pmatrix} \cos(\Phi) & -\sin(\Phi) \\ \sin(\Phi) & \cos(\Phi) \end{pmatrix} \begin{pmatrix} \cos(\Theta) - i\dfrac{\Gamma}{2\Theta}\sin(\Theta) & \dfrac{\Phi}{\Theta}\sin(\Theta) \\ -\dfrac{\Phi}{\Theta}\sin(\Theta) & \cos(\Theta) + i\dfrac{\Gamma}{2\Theta}\sin(\Gamma) \end{pmatrix} \begin{pmatrix} \cos\alpha_p \\ \sin\alpha_p \end{pmatrix}. \tag{7}$$

The transmitted light intensity is given by $T = |E_{\text{exit}}|^2$, or

$$T = \cos^2(\alpha_p - \alpha_a - \Phi) - \sin^2(\Theta)\sin(2\alpha_a)\sin[2(\alpha_p - \Phi)] - \frac{\Phi^2}{\Theta^2}\sin^2(\Theta)\cos[2(\alpha_p - \Phi)]\cos(2\alpha_a) - \frac{\Phi}{2\Theta}\sin(2\Theta)\sin[2(\alpha_p - \alpha_a - \Phi)]. \tag{8}$$

It is worthwhile to note that the last term of Eq. (8) depends linearly on Φ, which means that the left-hand (+) or right-hand (−) sense results in different transmittance profiles, depending on the arrangement of the polarizers, as shown by Eq. (8). One way to quantify this transmittance is to measure the spectrum with the wavelength of light. However, to fit the measured spectrum with the calculated one, it is necessary to know the dependence of the birefringence with wavelength, which can be expressed as follows [29]:

$$\Delta n(\lambda) = G\frac{\lambda^2\lambda^{\star 2}}{\lambda^2 - \lambda^{\star 2}}, \tag{9}$$

in which G is a temperature-dependent quantity related to the order parameter and $\lambda^\star$ is the mean wavelength of the UV absorption band. By combining Eqs. (9) and (8), one

can simulate the measured spectrum. Interestingly, if, for example, the HTP of a chiral dopant is known but the helical sense is not, one can use the set of equations described above to fit the spectrum, leaving the sign of Φ as a parameter. Similarly, these equations can be used to encounter the number of turns in twisted cells in a simple way.

III. EXPERIMENTAL SETUP

All the data presented in this paper with slab cells were taken from cells prepared in Kent State's clean-room facility. The ITO-coated glass was cleaned and coated with PI-2555 to generate homogeneous alignment, and the cells assembled after antiparallel rubbing and the chosen spacer (glass fiber) had been sprayed. All the cells were capillary filed, and the measurements were performed at room temperature. The wedge cell had spacers in the glue on only one side. To simultaneously compare the measured spectra with the one calculated from Eqs. (8) and (9), we developed a LabView program to acquire the data from an Ocean Optics USB4000 Spectrometer and adjust it with the model presented in the previous section. In all the cases studied here, the samples were placed in a polarizing light microscope (the spectrometer was coupled to the microscope). The reference spectrum was set by placing the polarizers parallel, while the background was set with crossed polarizers.

IV. SIMULATION AND EXPERIMENTAL RESULTS

A. Wavelength dependence of birefringence

For the first measurement, as a test, we measured the wavelength-dependent birefringence of a liquid-crystal cell. We filled a cell with a measured thickness of 10.0 μm using the nematic LC material E44 (Merck). The cell had antiparallel rubbing alignment and did not have an added chiral dopant, so there was no twist present in the cell ($\Phi = 0$). Indeed, a close inspection of Eq. (8) reveals that under the correct setting of polarizers and no twist, the equation reduces to the well-known transmission equation for a planar-oriented liquid-crystal cell reported in many textbooks [1,30]. The transmission spectrum of the sample was measured with the rubbing direction oriented at 45° between crossed polarizers. We substituted Eq. (9) into Eq. (8) and treated the constants G and $\lambda^\star$ as fitting parameters to match the experimentally measured transmission data to the calculated transmission data. The best-fit values found were $G = 3.428 \times 10^{-6}$ and $\lambda^\star = 251.7$ nm and the data is shown in Fig. 2. The value of Δn (589 nm) determined using the fit, 0.2657, is comparable to the literature value [31].

The power of the method can be further tested on samples containing chiral additives. For example, Eq. (8) can be used to measure the handedness of a twisted cell,

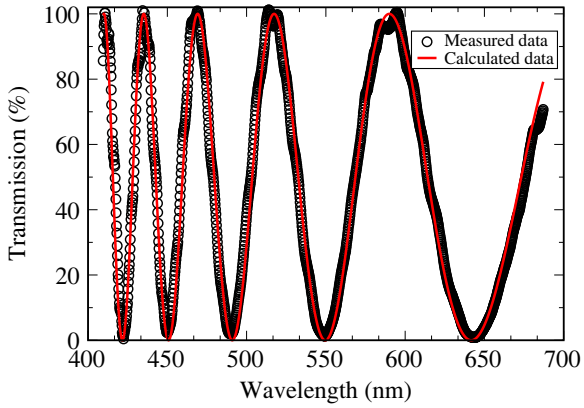

FIG. 2. Measured and calculated transmission data for the nematic cell.

which can be a simple twisted nematic or CLC cell. This kind of measurement is often helpful, for example, when another kind of chiral dopant is synthesized or characterized [24,25]. The twisted nematic (TN) display consists of liquid-crystal material that twists 90° from one substrate to the next. When the display is fabricated such that the twist matches the boundary conditions, then the electro-optic operation of the display becomes independent of the handedness (or direction) of the twist. However, the handedness of the chiral dopant must be known to make sure it matches the rubbing directions of the cell. This section demonstrates how measurement of the transmission spectrum of the cell is an accurate technique for determining the handedness (twist direction) of an unknown chiral dopant when the boundary conditions of the cell are known.

B. Determining twist handedness

First, as an example, we consider a case where the total twist angle is 2π. The symmetry of the transmission spectrum for a left- or right-handed twist can be broken by taking two measurements using different orientations of the analyzer. For example, two measurements can be done beginning with an arrangement that places the input rubbing direction of the sample (with unknown handedness) along the polarizing direction of the input polarizer. One measurement is taken with the analyzer rotated in the positive direction (right-handed), such as 20°, and the other measurement is taken after moving the analyzer in a negative direction (left-handed), such as −20°. By using the correct handedness in the calculated spectrum it will yield a good match to the measured data and the opposite handedness will not yield a good match. To clarify this point, Fig. 3 shows the transmission vs wavelength calculated with Eq. (8) for E7 when Φ is either positive or negative (right- or left-handed) and the angle α of the analyzer with the rubbing direction was of 20° or 45°, in all cases $|\Phi| = 2\pi$. When $\alpha = 20°$, the two-handedness behaves differently as depicted by the continuous (right-handed)

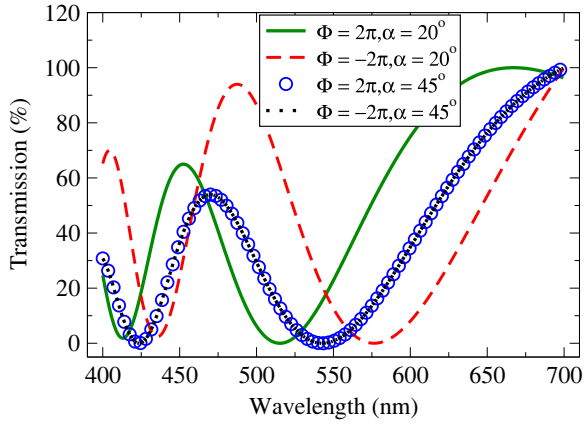

FIG. 3. Transmission vs wavelength calculated for E7 when Φ is either positive or negative (right- or left-handed) and the angle α is 20° or 45°.

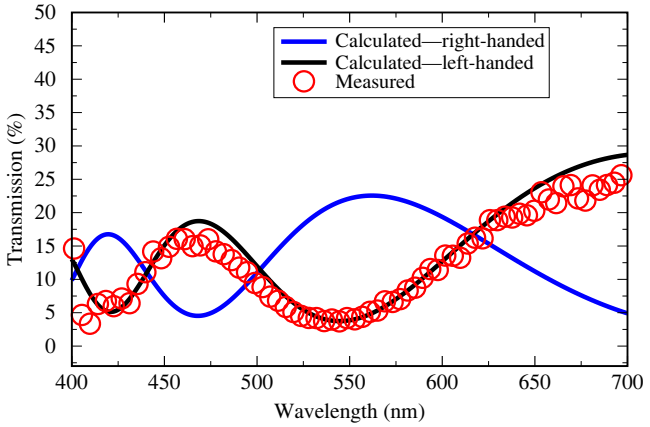

FIG. 4. Transmission as a function of wavelength for (R)-(+)-limonene. The black and blue solid lines represent the calculated data, while the red circle represents the measured data.

and the dashed (left-handed) curves. When $\alpha = 45°$, both spectra look the same and one cannot tell which one is right- or left-handed (dotted and circles).

In an experimental situation, the model presented here has been tested (although the details are presented here) before. In Ref. [25], the liquid crystal E44 was mixed with chiral dopant (R)-(+)-limonene at 3.9%, which has a measured HTP of $|2.6|\ \mu m^{-1}$ and filled into a 3.5 μm right-handed twisted cell whose inner surfaces had been coated with an alignment layer of PI-2555. The mixture was filled into a cell rubbed for a right-handed twist, but the pretilt angle was very low $\leq 2°$, which means the twist was more heavily influenced by the chiral dopant handedness. An applied voltage high enough to switch the cell was removed suddenly before the measurement because the liquid crystal first relaxes to the handedness induced by the chiral dopant. For the mentioned configuration, the spectrum is different if the sample is right- or left-handed and so we compared it with the calculated spectrum. As shown in Fig. 4, the calculated curve that fits the measured spectrum is left-handed [25]. Similarly, in Ref. [24], the model has been employed to prove that the alternative, photodriven axial chiral dopant was able to reverse the handedness of a CLC liquid crystal under UV illumination. With the previous knowledge of the HTP before and after UV irradiation, and measurement of the cell thickness before filling the cell, the spectra can be easily measured before and after UV illumination. The data were adjusted with Eqs. (9) and (8), and are shown in Fig. 6 of Ref. [24].

C. Determining the total twist angle

The proposed model can also be used to determine the number of turns in a long-pitch CLC. This is a very useful quantity because CLCs, when filled into a confined system such as a slab cell, will twist in a quantized way to satisfy the boundary conditions imposed by the alignment layer. Therefore, the number of turns may differ from what is expected from the knowledge of the HTP alone, and the CLC will have to pay an elastic penalty for the surface imposition. To test our model for counting the number of turns, we mixed the nematic LC material E44 (Merck) with 1.99% right-handed chiral dopant R811 (Merck). The liquid crystal was vacuum filled into a Cano-wedge cell where the pitch was measured to be 5.0 μm and the HTP was calculated to be $10.0\ \mu m^{-1}$. However, the Cano-wedge method determines the HTP using the slope angle of the wedge cell and the disclination line boundaries between Grandjean zones where it is assumed that an additional turn is inserted as the thickness increases. However, if more than one turn is inserted at a boundary, then the total number of turns in any particular zone (which depends on the pitch and the local cell gap) may not be the same as what is expected.

To gain further insights on Eq. (8), we used it to determine the number of turns. The cell gap of the Cano-wedge cell was measured as a function of position before the cell was filled, the measurement position was marked in the cell, and the results show it varied continuously from nearly zero to over 20.0 μm. After filling the cell, each Grandjean zone was identifiable between disclination lines. We made spectral measurements of each zone between crossed polarizers and when this data was compared to the calculated spectrum we were able to verify the number of turns in the liquid-crystal structure. For this procedure, we took the spectra as close as possible to the regions where the thickness (before filling with the liquid-crystal mixture) was measured; hence, the thickness associated with each spectrum was (approximately) known. We measured the first six regions. For the adjustment with the model, we left the number of turns and the cell thickness as fitting parameters, although the cell gap

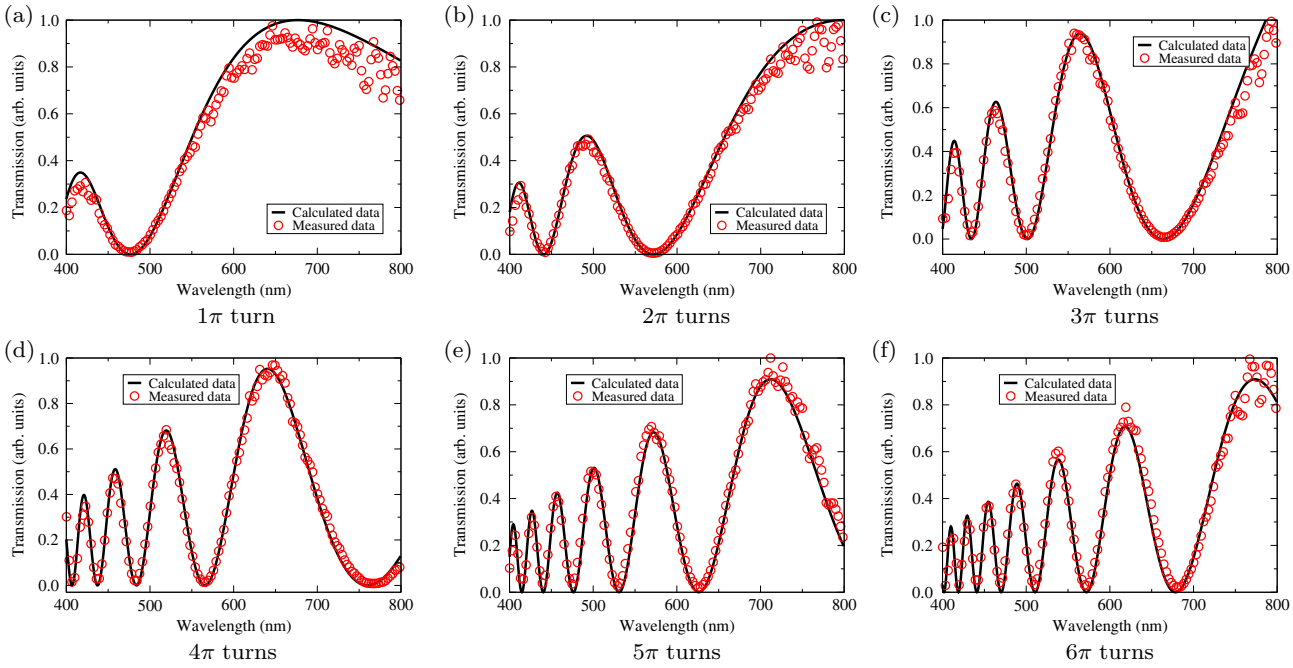

FIG. 5. Transmission vs wavelength measured for E44 + 1.99 % of R811 in a wedge cell. Each spectrum was measured in a position where the thickness was measured prior to filling the cell. We then used Eq. (8) to adjust the measured data by having the number of turns Φ and cell thickness as a fitting parameter. The thickness values found from the fit were close to the ones measured before filling the cell. (a) 1π turn, (b) 2π turns, (c) 3π turns, (d) 4π turns, (e) 5π turns, (f) 6π turns.

used was very close to the data measured prior to filling the cell. We used the G and $\lambda^\star$ obtained before. The measured and calculated spectra are shown in Fig. 5. It is noticeable how well the model adjusts the measured data. Figures 5(a) to 5(f) show the six measured zones. The thickness and number of turns obtained were, respectively: $d = 2.77$ μm and $\Phi = 1\pi$, $d = 4.79$ μm and $\Phi = 2\pi$, $d = 6.98$ μm and $\Phi = 3\pi$, $d = 9.43$ μm and $\Phi = 4\pi$, $d = 11.95$ μm and $\Phi = 5\pi$, $d = 14.38$ μm and $\Phi = 6\pi$. All the thicknesses we calculated are very close to the ones measured before and the number of turns are the ones expected for each Grandjean zone separating the integer number of π turns.

D. Terpenoids as chiral dopants

The terpenoids were acquired from Merck. (S)-(+)-carvone ($C_{10}H_{14}O$) is a liquid found mainly in caraway and dill seed oils and it is mainly used by the cosmetic industry. (1S)-(−)-verbenone ($C_{10}H_{14}O$) is also a liquid and it is one of the main components of the essential oil of *Suregada zanzibariensis* leaves [32] and it finds applications, among others, in the production of anti-ischemic materials [33]. The last chiral dopant is (3aR)-(+)-sclareolide ($C_{16}H_{26}O_2$), which is a powder derived from various plants, including *Salvia sclarea*, and it is used in the perfume industry and in the syntheses of some bioactive compounds [34].

We first mixed a small amount of each chiral dopant with the nematic host E7, placed it on a cover slip, and observed the mixture under POM. In all three cases, it was clear that the mixture became a CLC from the typical fingerprintlike texture of CLCs in contact with air [35]. We first measured the HTP of each material in E7 with the Grandjean-Cano wedge with a spherical lens method [1]. We prepared one sample for each material to get an estimate of the HTP value, but repeated the measurement with the lens at least three times to guarantee the sample's measurement is correct. The secondary measure of the handedness will later help to validate the HTP measurement. We used plane convex lenses with a radius of $R \sim 51.5$ mm and a focal length of 99.7 mm. Lenses and glass substrates were coated with an aqueous solution of 1% wt PVA that after deposition was prebaked for 1 min at 90 °C and then baked for 1 h at 120 °C. Both lens and glass substrates were rubbed and assembled in an antiparallel fashion with the rubbing direction, with the LC mixture sandwiched between them and analyzed under POM with a 4× objective. Since the thickness varies due to the curvature of the lens, the CLC structure increases the number of turns in half-pitch intervals, and a disclination line forms between regions with different numbers of turns. We then measured the distance of each line from the center of the lens, r_n, with the AmScope App. An example of defect lines and distance measurement is shown in Fig. 6(a), where the circles highlight the defect lines and the red lines

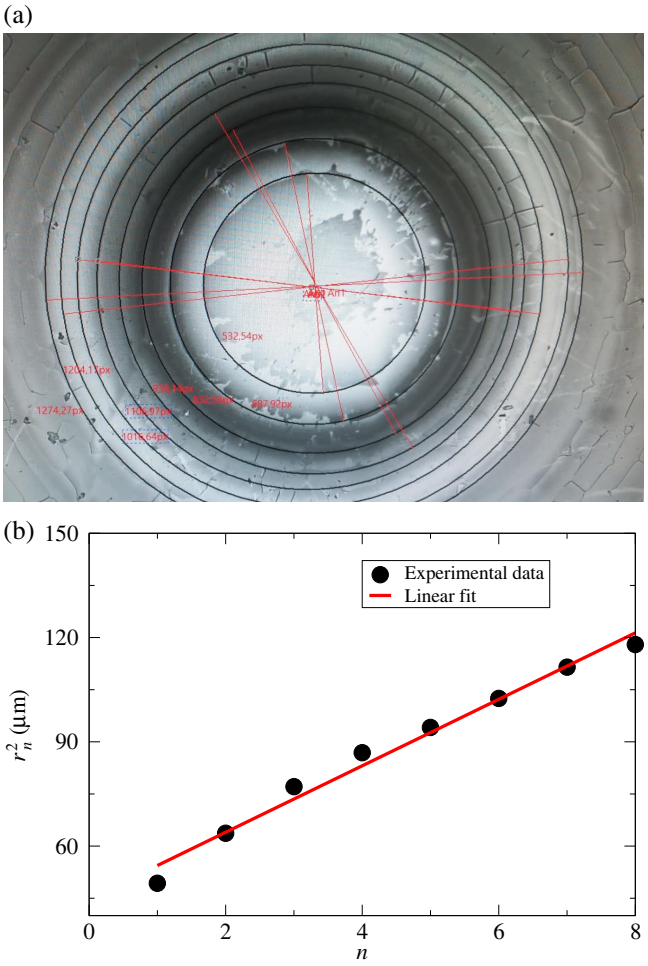

FIG. 6. (a) Example of POM image of the Grandjean zones used to measure the HTP of the terpenoids in E7. We used the software AmScope to highlight the disclination lines and calculate the distance. In (b), we show an example of the distance from the center square of each line against the line number and the linear fitting that results in the HTP of the material.

show the distance in pixels to the center. The curve r_n^2 vs n (where n refers to the nth line) shows a linear dependence and the slope of the curve $S = P_0 R$ [1], where P_0 is the pitch. If the concentration c is known, the HTP is found by the relation $\text{HTP} = 1/(cP_0)$ [1]. Figure 6(b) shows an example of the r_n^2 vs n curve and the linear fit to the experimental data.

We prepared the following samples (by weight) to measure the HTP: E7 + (3aR)-(+)-sclareolide 3.04%, E7 + (1S)-(−)-verbenone 5.74 % and E7 + (S)-(+)-carvone 3.14%. We then used the method described above to calculate the HTP of each material in E7. Absolute values are given in Table I. (S)-(+)-carvone has the highest absolute HTP, while (1S)-(−)-verbenone is the lowest. Although the three compounds have fairly low HTP, they are generally cheaper than commercially available chiral dopants, so they still find use in applications that require long pitch, such as in TN and STN cells [23].

TABLE I. Terpenoids used as chiral dopants in E7 host.

Material	|HTP|	Handedness
(3aR)-(+)-sclareolide	3.45	Right
(1S)-(−)-verbenone	0.58	Left
(S)-(+)-carvone	5.15	Left

To measure the helical sense of each compound in E7, we used the HTP values and fabricated CLC samples to have approximately 1π turn inside a slab cell treated to induce planar alignment with PI-2555. Since the HTPs of each component are different, we used different cell gaps for each material, to keep the concentration of chiral dopant low and therefore not induce too much change in the birefringence dispersion of E7. Since (3aR)-(+)-sclareolide is a powder, it is easy to prepare samples with relatively low concentrations of dopant. We thus prepared a sample of E7 + 1.47% of (3aR)-(+)-sclareolide, which produces a pitch of approximately 19.7 μm and filled this sample into a slab with a measured thickness of 9.8 μm. (S)-(+)-carvone is a liquid so it is a little trickier to prepare samples with low concentration. Hence, we made a sample of E7 + 2.20% of (S)-(+)-carvone, which produces a pitch of approximately 8.9 μm, and filled this sample into a slab of measured thickness of 5.3 μm. Lastly, (1S)-(−)-verbenone has a very low HTP, so it requires a large amount to produce a 1π turn sample in the slabs used for the other two samples. Thus, we prepared a sample of E7 + 4.4% of (1S)-(−)-verbenone, which results in a pitch of approximately 39.1 μm, and therefore we filled it into a slab of measured thickness of 18.8 μm. Therefore, all samples should have 1π turn (since PI-2555 promotes strong anchoring, the number of turns should always be an integer number of turns). Having all the other parameters of Eq. (8), and with Eq. (9) using $G = 2.9 \times 10^{-6}$ and $\lambda^\star = 249.1$ nm measured for E7, we collected the spectra for all three samples. The spectrometer was mounted in a POM where the polarizer angle $\alpha_p = 0^\circ$ and the analyzer angle $\alpha_a = 75^\circ$.

We then plotted in Fig. 7 along the spectrum for each material, the calculated spectrum using Eq. (8) for each sign of $|\Phi| = \pi$. Figures 7(a)–7(c) show the measured spectrum (open circles), and the calculated spectra for right- and left-handedness for (1S)-(−)-verbenone, (3aR)-(+)-sclareolide and (S)-(+)-carvone, respectively. For each case, we plot the curve that adjusted the measurement with the solid red line, and the opposite case in a solid blue line. Both (1S)-(−)-verbenone and (S)-(+)-carvone can only be adjusted by $\Phi = -\pi$, while (3aR)-(+)-sclareolide is only adjusted by $\Phi = \pi$. It is worthwhile to point out that for the three samples, the sign of Φ was the only parameter used to adjust Eq. (8), except for the

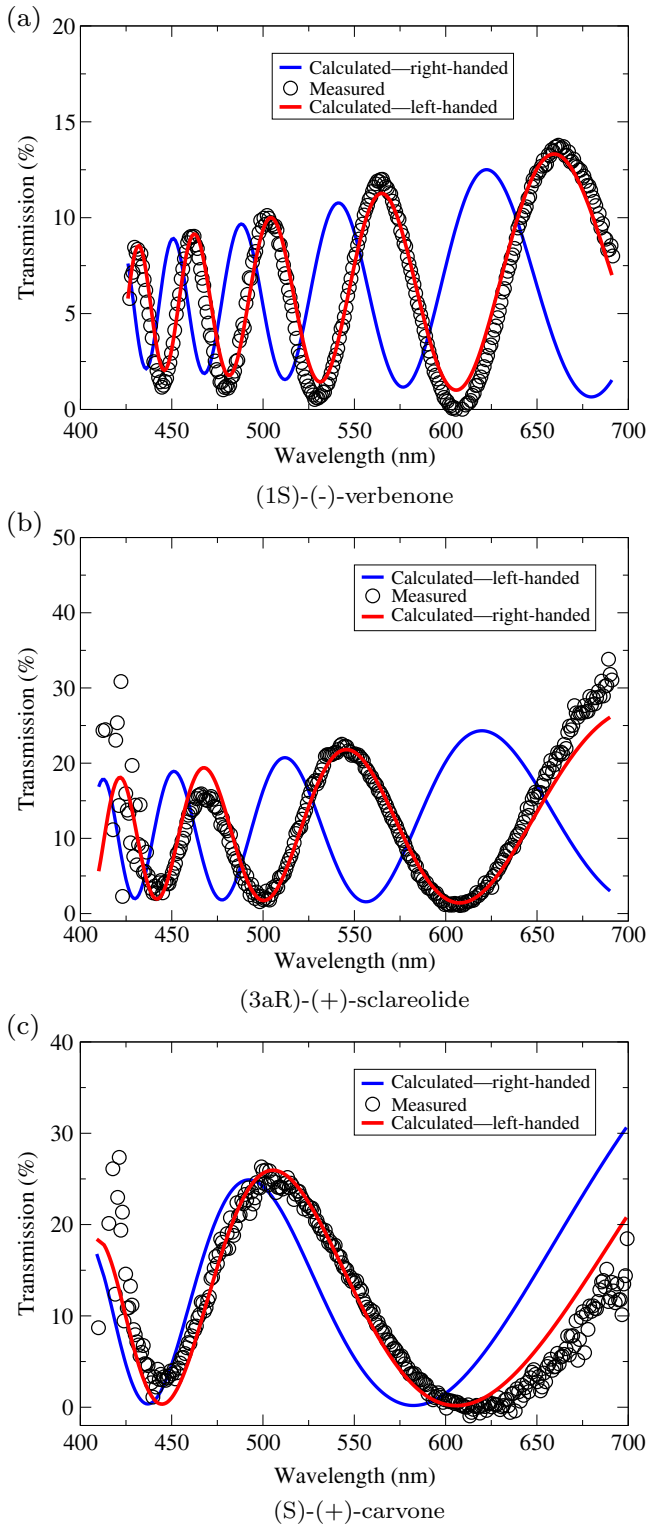

FIG. 7. Transmission vs wavelength for the three terpenoids used in this work as chiral dopants for E7. The open circles represent the measured data, while the solid red line represents the handedness that adjusts the data. The solid blue line represents the opposite handedness for comparison. (a) (1S)-(−)-verbenone (b) (3aR)-(+)-sclareolide (c) (S)-(+)-carvone.

(1S)-(−)-verbenone. Since the concentration for this case was considerably higher than that of the other dopants, the disordering effect caused by the non-nematogenic dopant is expressive, to the point that with 4.4% of (1S)-(−)-verbenone, the transition temperature of E7 decreases from approximately 58 °C to approximately 36 °C. Therefore, it reduces the birefringence of the material. Since we used the same G and $\lambda^\star$ for all fits, the decrease in retardance ϕ had to be compensated by slightly decreasing the value of the measured thickness, from $d = 19.3\ \mu\text{m}$ to $d \sim 17\ \mu\text{m}$, since $\phi \propto \Delta n/d$.

V. CONCLUSIONS

In conclusion, we demonstrated a simple method for obtaining several relevant parameters from the spectral measurements. We describe the main equations and propose the experimental situation for using the method. We showed that the measured transmission spectrum can be compared to the simulated spectrum to determine the twist sense (handedness) of a long-pitch twisted structure when the chiral dopant handedness is unknown, or it can also be used to verify the total number of turns in the structure whenever the handedness is known. In all cases, the cell gap must be known and measured before filling the cell. We then demonstrate its power in a series of simple experiments and in situations where it can be used with unknown chiral dopants, such as limonene, and to demonstrate helical inversion in a photosensitive chiral dopant.

We then tested three terpenoid materials, namely (1S)-(−)-verbenone, (3aR)-(+)-sclareolide, and (S)-(+)-carvone, as chiral dopants in the E7 liquid-crystal host. All the dopants have good miscibility with E7 and display the typical CLC texture upon mixing. We determined their HTPs with the Grandjean-Cano method with a spherical lens and used Eq. (8) to determine the handedness induced by each chiral dopant.

ACKNOWLEDGMENTS

This study was financed in part by the Coordenação de Aperfeiçoamento de Pessoal de Nível Superior – Brasil (CAPES) – Finance Code 001 (M.P.R.). E.K.L. thanks the partial financial support of the CNPq under Grant No. 301715/2022-0. R.S.Z. thanks the National Council for Scientific and Technological Development, CNPq, Process No. (304634/2020-4) and (465259/2014-6), the National Institute of Science and Technology Complex Fluids (INCT-FCx), and the São Paulo Research Foundation (FAPESP - 2014/50983-3).

[1] D. Yang and S. Wu, in *Wiley Series in Display Technology* (Wiley, Chichester, UK, 2014).

[2] D. Amabilino, *Chirality at the Nanoscale: Nanoparticles, Surfaces, Materials and More* (Wiley, Weinheim, Germany, 2009).

[3] R. S. Zola, L. R. Evangelista, Y.-C. Yang, and D.-K. Yang, Surface induced phase separation and pattern formation at the isotropic interface in chiral nematic liquid crystals, Phys. Rev. Lett. **110**, 057801 (2013).

[4] D. Demus, in *Handbook of Liquid Crystals* (Wiley, Weinheim, Germany, 1998).

[5] R. Eelkema and B. L. Feringa, Amplification of chirality in liquid crystals, Org. Biomol. Chem. **4**, 3729 (2006).

[6] T. J. White, R. L. Bricker, L. V. Natarajan, N. V. Tabiryan, L. Green, Q. Li, and T. J. Bunning, Phototunable azobenzene cholesteric liquid crystals with 2000 nm range, Adv. Funct. Mater. **19**, 3484 (2009).

[7] Z.-g. Zheng, R. S. Zola, H. K. Bisoyi, L. Wang, Y. Li, T. J. Bunning, and Q. Li, Controllable dynamic zigzag pattern formation in a soft helical superstructure, Adv. Mater. **29**, 1701903 (2017).

[8] L. Wang and Q. Li, Photochromism into nanosystems: Towards lighting up the future nanoworld, Chem. Soc. Rev. **47**, 1044 (2018).

[9] S. Furumi and N. Tamaoki, Glass-forming cholesteric liquid crystal oligomers for new tunable solid-state laser, Adv. Mater. **22**, 886 (2010).

[10] N. Y. Ha, Y. Ohtsuka, S. M. Jeong, S. Nishimura, G. Suzaki, Y. Takanishi, K. Ishikawa, and H. Takezoe, Fabrication of a simultaneous red–green–blue reflector using single-pitched cholesteric liquid crystals, Nat. Mater. **7**, 43 (2008).

[11] P. Raynes, S. J. Cowling, and J. W. Goodby, Investigations of optical activity of natural products and chiral pharmaceuticals using liquid crystal technologies, Anal. Methods **1**, 88 (2009).

[12] F. Zhai, Y. Feng, K. Zhou, L. Wang, Z. Zheng, and W. Feng, Graphene-based chiral liquid crystal materials for optical applications, J. Mater. Chem. C **7**, 2146 (2019).

[13] F. Grandjean, Sur l'existence de plans différenciés équidistants normaux à l'axe optique dans les liquides anisotropes (cristaux liquides), CR Seances Acad. Sci. Paris **172**, 71 (1921).

[14] R. Cano, in *Interprétation des Discontinuités de Grandjean*, Bulletin de Minéralogie Année, 91–1, pp. 20–27 (1968).

[15] M. Mitov, Cholesteric liquid crystals with a broad light reflection band, Adv. Mater. **24**, 6260 (2012).

[16] H. Hanson, A. Dekker, and F. Van der Woude, Analysis of the pitch in binary cholesteric liquid crystal mixtures, J. Chem. Phys. **62**, 1941 (1975).

[17] V. G. Guimarães, A. Svanidze, T. Guo, P. Nepal, R. J. Twieg, P. Palffy-Muhoray, and H. Yokoyama, Synthesis and characterization of novel bio-chiral dopants obtained from bio-betulin produced by a fermentation process, Crystals **11**, 785 (2021).

[18] P. R. Gerber, On the determination of the cholesteric screw sense by the Grandjean-Cano-method, Z. Naturforsch. A **35**, 619 (1980).

[19] H. Kozawaguchi and M. Wada, Helical sense and pitch of cholesteric liquid crystals, Mol. Cryst. Liq. Cryst. **45**, 55 (1978).

[20] J. Sato, N. Morioka, Y. Teramoto, and Y. Nishio, Chiroptical properties of cholesteric liquid crystals of chitosan phenylcarbamate in ionic liquids, Polym. J. **46**, 559 (2014).

[21] F. Tombolato, A. Ferrarini, and E. Grelet, Chiral nematic phase of suspensions of rodlike viruses: Left-handed phase helicity from a right-handed molecular helix, Phys. Rev. Lett. **96**, 258302 (2006).

[22] G. Zanchetta, F. Giavazzi, M. Nakata, M. Buscaglia, R. Cerbino, N. A. Clark, and T. Bellini, Right-handed double-helix ultrashort DNA yields chiral nematic phases with both right- and left-handed director twist, Proc. Natl. Acad. Sci. **107**, 17497 (2010).

[23] R. S. Zola, S. Hurley, and D.-K. Yang, D-limonene as a chiral dopant for thermotropic liquid crystalline systems, Appl. Phys. Express **4**, 061701 (2011).

[24] M. Mathews, R. S. Zola, S. Hurley, D.-K. Yang, T. J. White, T. J. Bunning, and Q. Li, Light-driven reversible handedness inversion in self-organized helical superstructures, J. Am. Chem. Soc. **132**, 18361 (2010).

[25] R. S. Zola, Y.-C. Yang, and D.-K. Yang, Limonene as a chiral dopant for liquid crystals: Characterization and potential applications, J. Soc. Inf. Disp. **19**, 410 (2011).

[26] T. Ohzono, T. Yamamoto, and J.-i. Fukuda, A liquid crystalline chirality balance for vapours, Nat. Commun. **5**, 3735 (2014).

[27] M. Nesterkina, O. Vashchenko, P. Vashchenko, L. Lisetski, I. Kravchenko, A. K. H. Hirsch, and C.-M. Lehr, Thermoresponsive cholesteric liquid—crystal systems doped with terpenoids as drug delivery systems for skin applications, Eur. J. Pharm. Biopharm. **191**, 139 (2023).

[28] R. Horn and C. Johnson, *Matrix Analysis* (Cambridge University Press, New York, 2013).

[29] S.-T. Wu, Birefringence dispersions of liquid crystals, Phys. Rev. A **33**, 1270 (1986).

[30] J. Friedel, M. Kleman, and O. Laverntovich, in *Partially Ordered Systems* (Springer New York, New York, 2013).

[31] F. Guérin, J.-M. Chappe, P. J. P. Joffre, and D. D. D. Dolfi, Modeling, synthesis and characterization of a millimeter-wave multilayer microstrip liquid crystal phase shifter, Jpn. J. Appl. Phys. **36**, 4409 (1997).

[32] E. Innocent, C. C. Joseph, N. K. Gikonyo, M. H. Nkunya, and A. Hassanali, Constituents of the essential oil of Suregada zanzibariensis leaves are repellent to the mosquito, Anopheles gambiae s.s., J. Insect Sci. **10**, 57 (2010).

[33] C. Ju, S. Song, S. Hwang, C. Kim, M. Kim, J. Gu, Y.-K. Oh, K. Lee, J. Kwon, K. Lee, W.-K. Kim, and Y. Choi, Discovery of novel (1S)-(−)-verbenone derivatives with anti-oxidant and anti-ischemic effects, Bioorg. Med. Chem. Lett. **23**, 5421 (2013).

[34] D. H. Hua, X. Huang, Y. Chen, S. K. Battina, M. Tamura, S. K. Noh, S. I. Koo, I. Namatame, H. Tomoda, E. M. Perchellet, and J.-P. Perchellet, Total syntheses of (+)-chloropuupehenone and (+)-chloropuupehenol and their analogues and evaluation of their bioactivities, J. Org. Chem. **69**, 6065 (2004).

[35] P. de Gennes and J. Prost, in *International Series of Monographs on Physics* (Clarendon Press, New York, 1993).